PP2A$^{B55\delta}$ Responsible for the High Initial Rates of Alcoholic Fermentation in Sake Yeast Strains of *Saccharomyces cerevisiae*

Daisuke Watanabe,[a,b#] Takuma Kajihara,[a] Yukiko Sugimoto,[a] Kenichi Takagi,[a] Megumi Mizuno,[b] Yan Zhou,[b] Jiawen Chen,[c] Kojiro Takeda,[d,e] Hisashi Tatebe,[a] Kazuhiro Shiozaki,[a] Nobushige Nakazawa,[f] Shingo Izawa,[g] Takeshi Akao,[b] Hitoshi Shimoi,[b,h] Tatsuya Maeda,[c]* Hiroshi Takagi[a]

[a]Division of Biological Science, Graduate School of Science and Technology, Nara Institute of Science and Technology, Ikoma, Nara, Japan

[b]National Research Institute of Brewing, Higashihiroshima, Hiroshima, Japan

[c]Institute of Molecular and Cellular Biosciences, the University of Tokyo, Tokyo, Japan

[d]Department of Biology, Faculty of Science and Engineering, Konan University, Kobe, Japan

[e]Institute for Integrative Neurobiology, Konan University, Kobe, Japan

[f]Department of Biotechnology, Faculty of Bioresource Science, Akita Prefectural University, Akita, Akita, Japan

[g]Graduate School of Science and Technology, Kyoto Institute of Technology, Kyoto, Japan.

[h]Faculty of Agriculture, Iwate University, Morioka, Iwate, Japan

Running title: PP2A$^{B55\delta}$ Drives Alcoholic Fermentation in Yeast

#Address correspondence to Daisuke Watanabe, d-watanabe@bs.naist.jp.

*Present address: Tatsuya Maeda, Department of Biology, Hamamatsu University School of Medicine, Hamamatsu, Shizuoka, Japan.

ABSTRACT

Sake yeast strain Kyokai no. 7 (K7) and its *Saccharomyces cerevisiae* relatives carry a homozygous loss-of-function mutation in the *RIM15* gene, which encodes a Greatwall-family protein kinase. Disruption of *RIM15* in non-sake yeast strains leads to improved alcoholic fermentation, indicating that the defect in Rim15p is associated with the enhanced fermentation performance of sake yeast cells. In order to understand how Rim15p mediates fermentation control, we here focused on target-of-rapamycin protein kinase complex 1 (TORC1) and protein phosphatase 2A with the B55δ regulatory subunit ($PP2A^{B55\delta}$), complexes that are known to act upstream and downstream of Rim15p, respectively. Several lines of evidence, including our previous transcriptomic analysis data, suggested enhanced TORC1 signaling in sake yeast cells during sake fermentation. Fermentation tests of the TORC1-related mutants using a laboratory strain revealed that TORC1 signaling positively regulates the initial fermentation rate in a Rim15p-dependent manner. Deletion of the *CDC55* gene encoding B55δ abolished the high fermentation performance of Rim15p-deficient laboratory yeast and sake yeast cells, indicating that $PP2A^{B55\delta}$ mediates the fermentation control by TORC1 and Rim15p. The TORC1-Greatwall-$PP2A^{B55\delta}$ pathway similarly affected the fermentation rate in the fission yeast *Schizosaccharomyces pombe*, strongly suggested that the evolutionarily conserved pathway governs alcoholic fermentation in yeasts. It is likely that elevated $PP2A^{B55\delta}$ activity accounts for the high fermentation performance of sake yeast cells. Heterozygous loss-of-function mutations in *CDC55* found in K7-related sake strains may indicate that the Rim15p-deficient phenotypes are disadvantageous to cell survival.

IMPORTANCE

The biochemical processes and enzymes responsible for glycolysis and alcoholic fermentation by the yeast *S. cerevisiae* have long been the subject of scientific research. Nevertheless, the factors determining fermentation performance *in vivo* are not fully understood. As a result, the industrial breeding of yeast strains has required empirical characterization of fermentation by screening numerous mutants through laborious fermentation tests. To establish a rational and efficient breeding strategy, key regulators of alcoholic fermentation need to be identified. In the present study, we focused on how sake yeast strains of *S. cerevisiae* have acquired high alcoholic fermentation performance. Our findings provide a rational molecular basis to design yeast strains with optimal fermentation performance for production of alcoholic beverages and bioethanol. In addition, as the evolutionarily conserved TORC1-Greatwall-PP2A$^{B55\delta}$ pathway plays a major role in the glycolytic control, our work may contribute to research on carbohydrate metabolism in higher eukaryotes.

KEYWORDS

Alcoholic fermentation, TORC1, Greatwall, Rim15p, PP2A$^{B55\delta}$, Cdc55p, sake yeast, *Saccharomyces cerevisiae*, *Schizosaccharomyces pombe*

INTRODUCTION

Sake, an alcoholic beverage made from fermented rice, typically has a higher alcohol content than beer or wine. During sake fermentation, saccharification by hydrolytic enzymes of *Aspergillus oryzae* and alcoholic fermentation by *Saccharomyces cerevisiae* sake yeast are the major bioconversions. Thus, the high alcohol content of sake is at least partly attributable to the unique characteristics of sake yeast. Sake yeast strains have long been selected based on the high fermentation performance, as well as the balanced production of aroma and flavor compounds (1, 2). Our previous comparative genomic and transcriptomic analyses revealed that a representative sake yeast, strain Kyokai no. 7 (K7), and its relatives carry a loss-of-function mutation in *RIM15* (*rim15*$^{5054\_5055insA}$), a gene of a highly conserved Greatwall-family protein kinase (3–5). Disruption of the *RIM15* gene in non-sake yeast strains, such as laboratory, beer, and bioethanol strains, leads to an increase in the fermentation rate (5–9), demonstrating that Rim15p inhibits alcoholic fermentation. Thus, the *rim15*$^{5054\_5055insA}$ mutation appears to be associated with the enhanced fermentation property of K7. Nevertheless, this loss-of-function mutation cannot be solely responsible for the sake yeast's improved fermentation, because expression of the functional *RIM15* gene does not suppress alcoholic fermentation in K7 (5). To better understand this phenomenon, the Rim15p-mediated fermentation control needs to be further dissected through comparative analysis between sake and non-sake yeast strains.

While Rim15p has been identified as a key inhibitor of alcoholic fermentation, involvement of the upstream regulators of Rim15p (Fig. S1) in fermentation control has not yet been fully examined. In *S. cerevisiae*, Rim15p activity is under the control of

several nutrient-sensing signaling protein kinases, including protein kinase A (PKA), the phosphate-sensing cyclin and cyclin-dependent protein kinase (CDK) complex termed Pho80p-Pho85p, and target-of-rapamycin protein kinase complex 1 (TORC1) (10, 11). Thus, inactivation of these kinases under nutrient starvation or other stress conditions may trigger Rim15p-dependent inhibition of alcoholic fermentation. Activation of TORC1 is mediated by the heterodimeric Rag GTPases (Gtr1p-Gtr2p in *S. cerevisiae*), which are negatively regulated by the Seh1p-associated protein complex inhibiting TORC1 (SEACIT) subcomplex (Iml1p-Npr2p-Npr3p in *S. cerevisiae*) that acts as a GTPase-activating protein for Gtr1p (12–14). Active TORC1 phosphorylates multiple targets including Sch9p, the yeast orthologue of the mammalian serum and glucocorticoid-regulated kinase (SGK) (15). Direct phosphorylation of Rim15p at Ser1061 by Sch9p contributes to sequestration of Rim15p in the cytoplasm, thereby inhibiting Rim15p functions (16). Recently, it was reported that the TORC1-Sch9p-Rim15p pathway is conserved and present in the evolutionarily distant fission yeast *Schizosaccharomyces pombe* (17), although it remains to be determined if the pathway affects the fermentation performance in this yeast species. In contrast, mammalian TORC1 (mTORC1) positively regulates glycolysis by the induction of glycolytic gene expression through hypoxia-inducible factor 1α (HIF1α) (18).

In *S. cerevisiae*, Rim15p targets the redundant transcription factors Msn2p and Msn4p (Msn2/4p) to mediate entry into the quiescent state (19, 20). In the context of fermentation control, Rim15p and Msn2/4p are required for the transcriptional induction of the UDP-glucose pyrophosphorylase-encoding gene *UGP1*, which switches the mode of glucose metabolism from glycolysis (a catabolic mode) to UDP-glucose synthesis (an

114 anabolic mode) (7). However, no orthologue of Msn2/4p has been found in other
115 organisms, and the role of the Greatwall-family protein kinases in carbohydrate
116 metabolism is unknown in *S. pombe* or higher eukaryotes. The Greatwall protein kinase
117 was originally identified as a potential cell cycle activator in *Drosophila* (21). In animals,
118 Greatwall directly phosphorylates a small protein called α-endosulfine (ENSA), which
119 inhibits the activity of protein phosphatase 2A accompanied by a regulatory subunit B55δ
120 ($PP2A^{B55\delta}$) (22, 23). Due to the antimitotic activity of $PP2A^{B55\delta}$, Greatwall is required for
121 maintenance of mitosis. More recently, the Greatwall-ENSA-$PP2A^{B55\delta}$ pathway was
122 reported to be conserved in *S. cerevisiae*; Rim15p phosphorylates ENSA orthologues
123 Igo1/2p to inhibit PP2A with the Cdc55p regulatory subunit (24–26). The orthologous
124 pathway has also been found in *S. pombe* and it plays a pivotal role in TORC1-mediated
125 cell cycle control (17). However, to our knowledge, the effect of $PP2A^{B55\delta}$ on
126 fermentation performance has not previously been described.

127 In the present study, we tested whether the TORC1-Greatwall-$PP2A^{B55\delta}$ pathway
128 participates in the control of alcoholic fermentation in *S. cerevisiae* and *S. pombe*. Our
129 results provide new insights into how yeast cells determine the mode of glucose
130 metabolism, especially in the context of the enhanced fermentation performance of sake
131 yeast strains.

132

133 **RESULTS**

134 **TORC1-associated transcriptomic profiles during alcoholic fermentation in**
135 **laboratory and sake yeast strains.** Our previous comparative transcriptomic analysis
136 indicated that the expression of the Rim15p- and Msn2/4p-targeted genes was attenuated

in K701 (a strain derived from K7) compared to that in the laboratory strain X2180 early in a 20-d sake fermentation test (3). This may be attributed not only to the sake yeast-specific loss-of-function mutation in the *RIM15* gene (*rim15*$^{5054\_5055insA}$; see also ref. 5), but also to higher TORC1 activity in the sake strains. TORC1 activity induces the ribosomal genes and the ribosome biogenesis genes, while it represses the nitrogen catabolite repression (NCR) and general amino acid control (GAAC) genes, as well as the Rim15p- and Msn2/4p-dependent stress-response genes (27) (Fig. S1). We found that these transcriptomic traits under the control of TORC1 are coordinated in common during sake fermentation. Although the Sfp1p-targeted genes encoding the ribosome-associated proteins in X2180 were rapidly downregulated during the progression of alcoholic fermentation, K701 cells maintained higher levels of these mRNAs at the initial stage of fermentation (Fig. 1A). Whereas the NCR and GAAC genes in X2180 were transiently upregulated early in sake fermentation, this transcriptional induction was not observed in K701 (Fig. 1B). Together, these data suggested that inactivation of TORC1 after the onset of alcoholic fermentation leads to attenuation of the Sfp1p-targeted gene expression and induction of the NCR and GAAC regulons in X2180. This phenomenon was less clearly observed in K701, implying a slower decline in TORC1 activity during the initial stage of alcoholic fermentation by K701.

To directly monitor TORC1 activity, an antibody against phospho-Thr737 of Sch9p (28) was used, as this TORC1-dependent phosphorylation of Sch9p is known to mediate signaling to Rim15p. Laboratory yeast and K701-lineage sake yeast cells engineered to overexpress 3HA-tagged Sch9p from a glycolytic gene promoter were sampled during alcoholic fermentation in YPD20 medium. The sake strain exhibited a

higher rate of carbon dioxide emission and completed alcoholic fermentation more rapidly than the laboratory strain (Fig. S2A). Phosphorylation of Sch9p Thr737 was detected only at the initial stage (at 6 h from the onset of alcoholic fermentation), and was more prominent in the sake strain than in the laboratory strain (Fig. S2B). The signals decayed quickly over time in both strains, suggesting that TORC1 activity is highest at the onset of alcoholic fermentation. It should be noted that the glycolytic promoter used in this study was inactivated after the completion of logarithmic phase (> 12 - 24 h) and 3HA-Sch9p was expressed only at low levels after 2 days.

Effects of the TORC1-Greatwall-PP2A$^{B55\delta}$ pathway on fermentation performance. In *S. cerevisiae* laboratory strains, loss of Rim15p leads to an increase in the initial rate of carbon dioxide emission during alcoholic fermentation (5, 7) (Fig. 2A). To examine whether TORC1 acts as a negative regulator of Rim15p activity in fermentation control, we tested the effect of altered TORC1 signaling on fermentation performance in a laboratory strain. Addition of a low concentration (1 nM) of the TORC1 inhibitor rapamycin to the medium led to a decrease in the rate of carbon dioxide emission from 1.5 d to 4 d (Fig. 2B). Since cell growth was not severely affected by 1 nM rapamycin (data not shown), the observed attenuation of carbon dioxide production was most likely indicative of reduced cellular fermentation performance. Deletion of the *TOR1* gene, which encodes a nonessential catalytic subunit of TORC1, also decreased carbon dioxide emission from 1.5 d to 3.5 d (Fig. 2C). Deletion of *TOR2*, which encodes a second TOR kinase that can also serve as a catalytic subunit of TORC1, was not tested in this study because Tor2p is essential for cell viability in *S. cerevisiae*. In contrast, the hyperactive *TOR1* and *TOR2* alleles (*TOR1*^{L2134M} and *TOR2*^{L2138M}) (28) increased carbon

183 dioxide emission around 1 d to 2 d (Figs. 2D and E). Strains harboring either of these
184 hyperactive alleles exhibited drastic decreases in the rate of carbon dioxide emission
185 toward the end of the fermentation tests. These results suggested that TORC1 activity
186 correlates with fermentation performance during the initial stage of the process. Indeed,
187 deletion of *GTR1* or *GTR2*, activators of TORC1 signaling, decreased carbon dioxide
188 emission (Figs. 2F and G). In addition, disruption of *NPR2* or *NPR3*, which encode the
189 components of the SEACIT subcomplex that inhibit TORC1 signaling, resulted in
190 increased carbon dioxide emission around 1.5 d to 2 d (Figs. 2H and I), corroborating the
191 role of TORC1 as a positive regulator of alcoholic fermentation. On the other hand, loss
192 of Sch9p, which mediates signaling between TORC1 and Rim15p (Fig. S1), markedly
193 decreased carbon dioxide emission (Fig. 2J).

194 Next, the effects of TORC1 on fermentation performance were examined in the
195 Rim15p-deficient strains. In *rim15*Δ cells of the laboratory strain, 1 nM rapamycin did
196 not affect carbon dioxide emission (Fig. 2K). We confirmed that the growth of *rim15*Δ
197 cells was not affected by 1 nM rapamycin (data not shown). In the *rim15*Δ background,
198 the hyperactive $TOR1^{L2134M}$ allele did not increase the initial rate of carbon dioxide
199 emission (1 - 2 d), but caused a decrease in the later stage of fermentation (> 3 d) (Fig.
200 2L). These data suggested that Rim15p is required for the TORC1-triggered fermentation
201 control, specifically in the early stage of alcoholic fermentation. Thus, it was predicted
202 that the fermentation performance of the sake strain defective in Rim15p is not affected
203 by TORC1 signaling. As expected, deletion of the *GTR1* or *SCH9* genes in the sake strain
204 did not change the maximum rate of carbon dioxide emission (Figs. 2M and N), although
205 alcoholic fermentation was slightly delayed in both cases, probably due to slower cell

growth. We also assessed whether the conserved TORC1-Greatwall pathway affects fermentation performance in the fission yeast *S. pombe*. As observed in budding yeast, an activated allele of *tor2*$^{+}$, *tor2*^{E2221K} (29), brought about increased carbon dioxide emission in fission yeast (Fig. 2O). Furthermore, deletion of the redundant Sch9p-orthologous genes, *sck1*$^{+}$ and *sck2*$^{+}$, resulted in decreased carbon dioxide emission (Fig. 2P).

Does Greatwall-triggered signaling to PP2A$^{B55\delta}$ play a role in the control of alcoholic fermentation? Deletion of the redundant ENSA-encoding genes *IGO1* and *IGO2* (*IGO1/2*), which mediate the signaling between Greatwall and PP2A$^{B55\delta}$ *in S. cerevisiae* (Fig. S1), led to an increased rate of carbon dioxide emission, as did deletion of *RIM15* (Figs. 3A and B). Similarly, in *S. pombe*, both the *cek1*Δ *ppk18*Δ and *igo1*Δ strains, which lack Greatwall and ENSA, respectively (17), exhibited higher rates of carbon dioxide emission than did the wild type (Figs. 3C and D). PP2A is a heterotrimeric enzyme complex composed of structural (A), regulatory (B), and catalytic (C) subunits. In budding yeast, the loss of both C subunit-encoding genes *PPH21* and *PPH22* leads to cell death, but disruption of either gene alone only weakly decreased carbon dioxide emission (Figs. 3E and F). In addition, deletion of the A subunit-encoding *TPD3* gene inhibited alcoholic fermentation (Fig. 3G). Moreover, deletion of *CDC55*, which encodes a B55δ-family regulatory subunit, severely decreased the rate of carbon dioxide emission throughout the duration of fermentation, whereas deletion of *RTS1* that encodes a B56-family regulatory subunit promoted alcoholic fermentation (Figs. 3H and I). In *S. pombe*, loss of the *ppa1*$^{+}$ or *ppa2*$^{+}$ gene, which encode C subunit isoforms, did not appear to affect alcoholic fermentation; however, loss of the *pab1*$^{+}$ gene encoding a B55δ subunit impaired alcoholic fermentation (Figs. 3J–L). Together, these data suggested that

the Greatwall-ENSA-PP2A$^{B55\delta}$ pathway is involved in the control of alcoholic fermentation in both *S. cerevisiae* and *S. pombe*. When combined with the Greatwall or ENSA defects, deletion of the *CDC55* (*S. cerevisiae*) or *pab1*$^{+}$ (*S. pombe*) genes almost fully canceled high fermentation performance (Figs. 3M–O). Thus, PP2A$^{B55\delta}$ is likely the major target of Greatwall and ENSA in the control of alcoholic fermentation in both yeasts.

Consistent with a previous report (5), expression of the functional *RIM15* gene derived from a laboratory strain did not attenuate alcoholic fermentation in the sake strain (Fig. 3P). Therefore, we next evaluated the role of PP2A$^{B55\delta}$ downstream of Rim15p in the high fermentation performance of sake yeast cells. Interestingly, we found that the diploid sake strain K701 is heterozygous for the deletion of a single adenine nucleotide at position 1092 of the *CDC55* gene (designated the *cdc55*^{MT} allele), resulting in a frameshift and premature polypeptide termination (Fig. 4A); thus, K701 carries only one functional *CDC55* allele (designated the *CDC55*^{WT} allele). To directly test the role of PP2A$^{B55\delta}$ in the sake yeast, the K701 strain was mutagenized by introduction of a *CDC55*-disrupting construct, yielding 12 heterozygous disruptants. Direct sequencing of the *CDC55* loci amplified from genomic DNA revealed that the *cdc55*^{MT} allele was disrupted in six of the heterozygous disruptants, while the *CDC55*^{WT} allele was disrupted in the other six heterozygous disruptants. The former class, in which the *CDC55*^{WT} allele remains intact, exhibited fermentation characteristics similar to the parental K701 strain (Fig. 3Q), while the latter class with no functional *CDC55* gene exhibited markedly lower carbon dioxide emission, especially in the initial stage of fermentation (0.5 - 2 d) (Fig. 3R). These results indicated that the *CDC55*^{WT} allele is required for the high fermentation

252 performance of the K701 sake yeast strain.

253 **Heterozygous nonsense or frameshift mutations in the *CDC55* gene of the**
254 **sake yeast strains.** As mentioned above, we identified a heterozygous loss-of-function
255 mutation (*cdc55*^{1092delA}) in diploid K701 (Fig. 4A). To test whether this mutation is
256 conserved among the sake strains, we analyzed the sequence of the *CDC55* genes in 17
257 K7-related Kyokai sake strains, including K6, K601, K7, K701, K9, K901, K10, K1001,
258 K11, K12, K13, K14, K1401, K1501, K1601, K1701, and K1801 [Note that the
259 numbering corresponds to the sequential isolation of these strains. The "-01" suffix is
260 used to indicate foamless variants that do not generate thick foam layers during sake
261 fermentation; for instance, K701 is the foamless variant of K7 (30).]. As shown in Fig. 4B,
262 the *cdc55*^{1092delA} mutation is unique to K701, and 65% (11 of 17) of the tested strains
263 contain other nonsense or frameshift mutations in the open reading frame of the *CDC55*
264 gene. Notably, the three most recently isolated strains, K1601, K1701, and K1801, have
265 neither a nonsense mutation nor a frameshift mutation in this locus. Although there are a
266 few lineage-specific mutations, such as *cdc55*^{C793T} in K10 and K1001 and *cdc55*$^{351\_352insA}$
267 in K7 and K1501 (2), closely associated strains do not always contain the same mutation
268 (e.g., K6 versus K601, K7 versus K701, or K7 versus K11). Each year, every Kyokai sake
269 yeast strain was selected from clone stocks before distribution by the Brewing Society of
270 Japan; notably, the K7 strains from three different years (1970, 1972, and 1974) carry
271 distinct *cdc55* mutations. The K7 strain used for whole-genome analysis (4) harbors a
272 *cdc55* mutation identical to the *cdc55*^{1571delC} allele in K7_1970. Thus, it appears that most
273 of the *cdc55* mutations represent independent events that occurred after the establishment
274 of the individual sake strains. While the *cdc55*^{1571delC} mutation in K7_1974 results in

additional 27 amino acid residues at the carboxyl terminus of the encoded protein, each of the other frameshift mutations leads to a premature stop codon that truncates the carboxyl terminus. Since all of the identified mutations are heterozygous, the effects of the *cdc55* loss-of-function mutations may be masked by the functional *CDC55* allele, as observed in K701.

Effects of PP2A$^{B55\delta}$ on the intracellular levels of glycolytic intermediates. Since PP2A$^{B55\delta}$ dephosphorylates many cellular substrates (31), it is difficult to infer how PP2A$^{B55\delta}$ controls alcoholic fermentation. However, it may be worth examining whether PP2A$^{B55\delta}$ regulates the activities of carbon metabolic enzymes through protein dephosphorylation as several recent studies have shed light on posttranslational modification as regulatory mechanisms for metabolic flux *in vivo* (32, 33). In the present study, we adopted a metabolomic approach to explore the glycolytic reactions that may be affected by the loss of PP2A$^{B55\delta}$ function. Metabolites were extracted from cells sampled at the early stages (6 h, 1 d, or 2 d) of alcoholic fermentation in YPD20 medium. Relative metabolite levels at 6 h indicated that the pools of early glycolytic intermediates [glucose 6-phosphate (G6P), fructose 6-phosphate (F6P), fructose 1,6-bisphosphte (F1,6BP), and dihydroxyacetone phosphate (DHAP)] were slightly increased by deletion of the *CDC55* gene in the laboratory strain BY4741 (Fig. 5A). In contrast, the level of glyceraldehyde 3-phosphate (G3P) accumulated in *cdc55*Δ cells was 3-fold higher than that in wild-type cells, while the intracellular pools of 3-phosphoglyceric acid (3PG) and the ensuing glycolytic intermediates were smaller in *cdc55*Δ cells. These data suggest that, at 6 h, the metabolic steps between G3P and 3PG are specifically compromised by deletion of the *CDC55* gene. We noted that 1,3-bisphosphoglyceric acid (1,3BPG), an

298 intermediate between G3P and 3PG in the glycolytic pathway, was not detected in both
299 wild-type and *cdc55*Δ cells in the present analysis. At 1 d, similar accumulations were
300 observed for F6P and phosphoenolpyruvic acid (PEP) in *cdc55*Δ cells (Fig. 5B); the
301 accumulation of F6P remained even at 2 d (Fig. 5C). These data suggested that, at 1 - 2 d,
302 the metabolic steps between F6P and F1,6BP, and between PEP and pyruvic acid, are
303 disturbed by deletion of the *CDC55* gene. In the sake strain K701 at 1 d from the onset of
304 alcoholic fermentation, the accumulations of F6P and PEP were observed in
305 $CDC55^{WT}$-deficient cells ($cdc55^{WT}\Delta/cdc55^{MT}$) (Fig. 5D), consistent with the results
306 obtained using laboratory yeast cells. Based on these results, it is possible to hypothesize
307 that the enzymatic activities of phosphofructokinase (F6P to F1,6BP) and/or pyruvate
308 kinase (PEP to pyruvic acid) are negatively affected by the loss of $PP2A^{B55\delta}$ function both
309 in laboratory and sake strains, when the fermentation rates reach their maxima.
310
311 **DISCUSSION**
312 Although the genes and enzymes of the glycolysis and alcoholic fermentation pathways
313 have been thoroughly studied in *S. cerevisiae*, the mechanisms by which intracellular
314 signaling pathways regulate carbohydrate metabolism in response to extracellular cues
315 are still not fully elucidated. We previously identified a loss-of-function mutation in the
316 *RIM15* gene ($rim15^{5054\_5055insA}$) that is present in K7 and shared among the associated
317 sake yeast strains, indicating that this mutation is associated with enhanced fermentation
318 performance (5, 7). In the present work, we showed that sake yeast cells exhibit elevated
319 TORC1 activity during alcoholic fermentation in comparison to laboratory strains.
320 TORC1 upregulates the Sfp1p-targeted genes encoding ribosome-associated proteins and

downregulates members of the NCR and GAAC regulons in a Rim15p-independent manner (27). These attributes (Fig. 1), as well as the observed defect in induction of the Msn2/4p-mediated stress-response genes (3), suggest enhanced activation of TORC1 in sake yeast cells (compared to laboratory strains). The high level of phosphorylated Thr737 of Sch9p observed in sake yeast cells (Fig. S2) is consistent with this idea. As previously reported, TORC1 activity is not fully attenuated in K7 cells even under nitrogen limitation (34). Therefore, elevated TORC1 activity can be regarded as a novel hallmark of the sake yeast cells. In general, nutritional limination and environmental stresses rapidly inactivate TORC1 in yeast, resulting in inhibition of cell growth and proliferation. We postulate that the maintenance of high TORC1 activity in sake yeast cells may facilitate cellular metabolic activity even under fermentative conditions. Among the components of TORC1, only Tor1p contains missense mutations (R167Q and T1456I) in K7 and its relatives. Further studies will be needed to evaluate the roles of the mutations in *TOR1* and those in other genes to be discovered in sake yeast strains.

In the present study, we demonstrated that the conserved TORC1-Greatwall-PP2A$^{B55\delta}$ pathway is key to the control of alcoholic fermentation (Fig. 6A). In *S. cerevisiae* laboratory strains and *S. pombe*, altered TORC1 activities led to changes in fermentation performance, specifically at the early stage of alcoholic fermentation. However, in laboratory yeast cells deficient for Greatwall, the initial rate of alcoholic fermentation was maintained and not affected by changes in TORC1. In contrast, in PP2A$^{B55\delta}$-deficient laboratory yeast cells, the fermentation rate was strikingly low and not enhanced even by a loss of Greatwall or ENSA. The observed strong epistasis suggested that the Greatwall-PP2A$^{B55\delta}$ pathway, among numerous downstream

344 effector proteins of TORC1, is the primary mediator of fermentation control. This
345 epistasis also indicated that PP2A$^{B55\delta}$ is the major regulator of the alcoholic fermentation
346 machinery.

347 In our hypothesis, both high TORC1 activity and loss of Rim15p contribute to
348 the activation of PP2A$^{B55\delta}$ and the subsequent enhancement of the cellular fermentation
349 performance in the K7-related sake strains (Fig. 6B). Indeed, neither impairment of
350 TORC1 nor recovery of Rim15p is sufficient to attenuate PP2A$^{B55\delta}$ activity in these cells.
351 Presumably, even if TORC1 activity is decreased, the change in TORC1 signaling may
352 not be conveyed downstream due to the loss of Rim15p (Fig. S1). On the other hand, if a
353 functional *RIM15* gene is restored, the hyperactivated TORC1 can inhibit the functions of
354 Rim15p, resulting in elevated PP2A$^{B55\delta}$ activity. Our data indicated that the high
355 fermentation performance of sake yeast cells was abrogated only when the functional
356 *CDC55* (B55δ-encoding) gene was disrupted (Fig. 3R). Consequently, the two changes
357 (in TORC1 and Rim15p) observed in the TORC1-Greatwall-PP2A$^{B55\delta}$ pathway of sake
358 yeast cells may mutually ensure the robust phenotype of these strains in the context of
359 alcoholic fermentation.

360 Why do multiple sake yeast strains possess putative loss-of-function mutations
361 (i.e., nonsense mutations and frameshift mutations; Fig. 4B) in the *CDC55* gene? Since
362 diploid sake yeast strains contain two copies of the *CDC55* gene, heterozygosity for a
363 loss-of-function mutation at the loci may not yield apparent effects on alcoholic
364 fermentation. PP2A$^{B55\delta}$ regulates not only carbohydrate metabolism but also cell cycle
365 progression. In *S. cerevisiae*, PP2A$^{B55\delta}$ is the key inhibitor of the entry into quiescence
366 (G_0 phase). Loss of Rim15p decreases the expression of stress-response genes and

367 shortens chronological life span, and *cdc55*Δ is able to suppress such Rim15p-deficient
368 phenotypes (24). The heterozygous loss-of-function mutations in *CDC55* in the sake
369 strains may reduce the dosage of functional Cdc55p, thereby serving as weak suppressors
370 of the long-term survival defect associated with the $rim15^{5054\_5055insA}$ mutation (Fig. S3).
371 Another mutation in the functional *CDC55* allele or a loss of heterozygosity (LOH) may
372 further enhance cell viability, although the lack of Cdc55p function severely impairs
373 fermentation performance. Thus, the individual sake strains may have independently
374 acquired and maintained the heterozygous *cdc55* mutations during decades of selection
375 for enhanced fermentation. Based on our model, we propose that the *cdc55* mutations
376 identified in the sake strains are potential fermentation inhibitors whose elimination could
377 facilitate the development of genetically stable sake yeast strains.

378 Comparison of the glycolytic intermediate pools between wild-type and *cdc55*Δ
379 cells suggested that the loss of $PP2A^{B55\delta}$ negatively affects the metabolic reactions
380 responsible for the conversion of (i) F6P to F1,6BP, (ii) G3P to 3PG, and (iii) PEP to
381 pyruvic acid during the initial stage of alcoholic fermentation (Fig. 5). We presume that
382 these defects are at least partially responsible for the low fermentation performance of
383 *cdc55*Δ cells. Intriguingly, $PP2A^{B55\delta}$ appears to control individual glycolytic reactions in
384 a fermentation-phase-specific manner; only the defect in (ii) was observed at 6 h from the
385 onset of alcoholic fermentation in a laboratory strain, whereas the defects of (i) and/or
386 (iii) were observed from 1 d to 2 d. Thus, these results imply that the activities of
387 glycolytic enzymes are separately regulated during alcoholic fermentation, and that the
388 pleiotropic functions of $PP2A^{B55\delta}$ contribute to the optimal glycolytic flux. Among the
389 glycolytic enzymes, phosphofructokinase and pyruvate kinase catalyze irreversible and

rate-limiting reactions, (i) and (iii), respectively, in glycolysis. Recent integrated phosphoproteomics data in budding yeast indicate that Pfk1p and Pfk2p (the α and β subunits of phosphofructokinase, respectively) and Cdc19p (the main pyruvate kinase isozyme) form phosphorylation hubs, suggesting that multiple protein kinases phosphorylate these enzymes to modulate their activity, intracellular localization, or protein degradation (32, 33). For example, it has been reported that phosphorylation of residue Ser163 of Pfk2p inhibits the phosphofructokinase activity *in vivo* under gluconeogenic conditions (35). The protein phosphatase activity of $PP2A^{B55\delta}$ may directly regulate glycolytic enzymes by counteracting such inhibitory phosphorylation. In fact, Pfk1p and Pfk2p are listed as putative $PP2A^{B55\delta}$-dephosphorylated proteins (31). The 3PG kinase Pgk1p, which is involved in reaction (ii), also is a putative $PP2A^{B55\delta}$ target. The phosphorylation status and the activities of the candidate enzymes should be compared between wild-type and *cdc55*Δ cells during alcoholic fermentation. Since the glycolytic pathway and the posttranslational modifications of the glycolytic enzymes are often conserved evolutionarily, our study may also offer clues to identify novel key mechanisms of protein phosphorylation-mediated glycolytic control by the TORC1-Greatwall-$PP2A^{B55\delta}$ pathway.

MATERIALS AND METHODS

Yeast strains. The yeast strains used in this study are listed in Table S1. *Saccharomyces cerevisiae* laboratory strain BY4741 and its single-deletion mutants were obtained from Euroscarf (Germany). Another *S. cerevisiae* laboratory strain X2180 and *Schizosaccharomyces pombe* wild-type strain 972 were obtained from the American Type

413 Culture Collection (ATCC, USA). Sake yeast strains Kyokai no. 7 (K7) and its relatives
414 (K6, K601, K701, K9, K901, K10, K1001, K11, K12, K13, K14, K1401, K1501, K1601,
415 K1701, and K1801) were provided by the Brewing Society of Japan (BSJ, Japan). *S.*
416 *pombe* strain ED666 *cek1*Δ*::kanMX* (*h*$^{+}$ *ade6-M210 ura4-D18 leu1-32 cek1*Δ*::kanMX*)
417 was obtained from Bioneer (Korea).

418 Disruption of the *IGO2* gene in BY4741 *igo1*Δ was performed using a
419 PCR-based method (36) with a gene-specific primer pair and plasmid pFA6a-hphNT (37)
420 as the template to generate BY4741 *igo1*Δ*::kanMX igo2*Δ*::hphNT* (*igo1/2*Δ). Disruption
421 of the *CDC55* gene in BY4741 wild type, BY4741 *rim15*Δ and BY4741 *igo1/2*Δ was
422 performed using a PCR-based method (36) with a gene-specific primer pair and plasmid
423 pFA6a-natNT (37) as the template to generate BY4741 *cdc55*Δ*::natNT* (*cdc55*Δ),
424 BY4741 *cdc55*Δ*::natNT rim15*Δ*::kanMX* (*cdc55*Δ *rim15*Δ), and BY4741 *cdc55*Δ*::natNT*
425 *igo1*Δ*::kanMX igo2*Δ*::hphNT* (*dc55*Δ *igo1/2*Δ), respectively.

426 The *TOR1*^{L2134M} mutation was previously reported as a hyperactive point
427 mutation in the kinase domain of Tor1p (28). Since the mutation site was conserved in the
428 *TOR2* gene, the corresponding mutation was also introduced to generate *TOR2*^{L2138M}.
429 Disruption of the *RIM15*, *GTR1*, *GTR2*, and *SCH9* genes in TM142 wild type or in
430 TM142 *TOR1*^{L2134M} was performed using a PCR-based method (36) with a gene-specific
431 primer pair and plasmid pFA6a-kanMX (37) as the template to generate TM142
432 *rim15*Δ*::kanMX* (*rim15*Δ), TM142 *TOR1*^{L2134M} *rim15*Δ*::kanMX* (*TOR1*^{L2134M} *rim15*Δ),
433 TM142 *gtr1*Δ*::kanMX* (*gtr1*Δ), TM142 *gtr2*Δ*::kanMX* (*gtr2*Δ), and TM142
434 *sch9*Δ*::kanMX* (*sch9*Δ), respectively.

435 Heterozygous disruption of the *CDC55* gene in K701 was performed using a

436 PCR-based method (36) with a gene-specific primer pair and plasmid pFA6a-natNT (37)
437 as the template. Correct disruption of the *CDC55*^{WT} or *cdc55*^{MT} allele was confirmed by
438 genomic PCR and direct DNA sequencing of the PCR product. Homozygous disruption
439 of the *SCH9* gene in IB1401 was performed according to a previous report (32). To
440 overexpress 3HA-tagged Sch9p from a glycolytic gene promoter in IB1401, plasmid
441 p416-3HA-SCH9 (kindly gifted from Prof. Kevin Morano from the University of Texas,
442 USA) was introduced into IB1401.

443 Disruption of the *ppk18*$^{+}$ and *igo1*$^{+}$ genes in 972 wild type was performed using
444 a PCR-based method (36) with a gene-specific primer pair and plasmid pFA6a-kanMX
445 (37) as the template to generate 972 *ppk18*Δ*::kanMX* and 972 *igo1*Δ*::kanMX* (*igo1*Δ),
446 respectively. The *kanMX* genes in ED666 *cek1*Δ*::kanMX* and 972 *ppk18*Δ*::kanMX* were
447 replaced with *natMX* and *hphMX*, respectively, using a one-step marker switch (38) to
448 generate ED666 *cek1*Δ*::natMX* and 972 *ppk18*Δ*::hphMX*, respectively. Both strains were
449 mated and sporulated to generate the prototrophic double mutant *cek1*Δ*::natMX*
450 *ppk18*Δ*::hphMX* (*cek1*Δ *ppk18*Δ). To construct the prototrophic mutants *sck1*Δ*::his7*$^{+}$
451 *sck2*Δ*::ura4*$^{+}$ (*sck1*Δ *sck2*Δ), *ppa1*Δ*::ura4*$^{+}$ (*ppa1*Δ), *ppa2*Δ*::ura4*$^{+}$ (*ppa2*Δ), and
452 *pab1*Δ*::ura4*$^{+}$ (*pab1*Δ), a suitable wild-type strain was mated with JX766 (39), MY1121,
453 MY1122 (40), and MY7214 (41), respectively, and sporulated. The *pab1*Δ and *igo1*Δ
454 strains were mated and sporulated to generate the prototrophic double mutant
455 *pab1*Δ*::ura4*$^{+}$ *igo1*Δ*::kanMX* (*pab1*Δ *igo1*Δ).

456 Yeast cells were routinely grown in liquid YPD medium (1% yeast extract, 2%
457 peptone, and 2% glucose) at 30°C, unless stated otherwise.

458 **Sequencing of the *CDC55* gene.** To analyze the *CDC55* sequence, the gene was

459 amplified by PCR with the primer pair CDC55-(-150)-F (5'-GGC AGC TTA ATA
460 CGA TTA CCC C-3') and CDC55-(+1906)-R (5'-TGG TGA AGT GAT
461 GAA AGA AGT CC-3'), using genomic DNA from the strain of interest as the
462 template. The PCR product was sequenced directly using a BigDye terminator v3.1 cycle
463 sequencing kit (Thermo Fisher Scientific) and primers CDC55-seq2 (5'-TCG AGG
464 TCA AAC TGG AGA GA-3'), CDC55-seq3 (5'-AAA ATC ATT GCT
465 GCC ACC CC-3'), and CDC55-seq4 (5'-TGA TAC CTA TGA AAA CGA
466 TGC GA-3') on a 3130xl Genetic Analyzer (Applied Biosystems); sequencing was
467 performed at Fasmac Co., Ltd. (Japan).

468 **Fermentation tests.** For measurements of fermentation rates, yeast cells were
469 precultured in YPD medium at 30°C overnight, inoculated into 50 mL of YPD20 medium
470 (1% yeast extract, 2% peptone, and 20% glucose) for *S. cerevisiae* or YPD10 medium
471 (1% yeast extract, 2% peptone, and 10% glucose) for *S. pombe* at a final optical density at
472 a wavelength of 600 nm (OD_{600}) of 0.1, and then further incubated at 30°C without
473 shaking. Fermentation progression was continuously monitored by measuring the volume
474 of evolved carbon dioxide gas using a Fermograph II apparatus (Atto) (42).

475 **Analysis of intracellular metabolite profiles.** During the fermentation tests in
476 YPD20 medium, yeast cells corresponding to an OD_{600} of 20 were collected at 6 h, 1 d, or
477 2 d from the onset of the fermentation tests. All pretreatment procedures for the samples
478 were performed according to the protocols provided by Human Metabolic Technologies,
479 Inc. Briefly, each sample of yeast cells was washed twice with 1 mL ice-cold Milli-Q
480 water, suspended in 1.6 mL methanol containing 5 μM internal standard solution 1
481 (Human Metabolic Technologies), and then sonicated for 30 s at room temperature.

Cationic compounds were measured in the positive mode of CE-TOFMS, and anionic compounds were measured in the positive and negative modes of CE-MS/MS (43). Peaks detected by CE-TOFMS and CE-MS/MS were extracted using automatic integration software (MasterHands, Keio University (44) and MassHunter Quantitative Analysis B.06.00, Agilent Technologies, respectively) to obtain peak information, including *m/z*, migration time, and peak area. The peaks were annotated with putative metabolites from the HMT metabolite database (Human Metabolic Technologies) based on their migration times in CE and *m/z* values as determined by TOFMS and MS/MS. Metabolite concentrations were calculated by normalizing the peak area of each metabolite with respect to the area of the internal standard and by using standard curves, which were obtained from three-point calibrations.

ACKNOWLEDGEMENTS

The Japan Society for the Promotion of Science (JSPS) provided funding to DW under grant number 16K18676, to SI under grant number 17H03795, and to TM under grant numbers 25291042 and 17H03802. The Public Foundation of Elizabeth Arnold-Fuji provided funding to DW. The Foundation for the Nara Institute of Science and Technology provided funding to DW. The authors declare no conflicts of interest.

REFERENCES

1. Kitagaki H, Kitamoto K. 2013. Breeding research on sake yeasts in Japan: history, recent technological advances, and future perspectives. Annu Rev Food Sci Technol 4:215–235.
2. Ohnuki S, Okada H, Friedrich A, Kanno Y, Goshima T, Hasuda H, Inahashi M, Okazaki N, Tamura H, Nakamura R, Hirata D, Fukuda H, Shimoi H, Kitamoto K, Watanabe D, Schacherer J, Akao T, Ohya Y. 2017. Phenotypic diagnosis of lineage and differentiation during sake yeast breeding. G3 (Bethesda) 7:2807–2820.
3. Watanabe D, Wu H, Noguchi C, Zhou Y, Akao T, Shimoi H. 2011. Enhancement of the initial rate of ethanol fermentation due to dysfunction of yeast stress response components Msn2p and/or Msn4p. Appl Environ Microbiol 77:934–941.
4. Akao T, Yashiro I, Hosoyama A, Kitagaki H, Horikawa H, Watanabe D, Akada R, Ando Y, Harashima S, Inoue T, Inoue Y, Kajiwara S, Kitamoto K, Kitamoto N, Kobayashi O, Kuhara S, Masubuchi T, Mizoguchi H, Nakao Y, Nakazato A, Namise M, Oba T, Ogata T, Ohta A, Sato M, Shibasaki S, Takatsume Y, Tanimoto S, Tsuboi H, Nishimura A, Yoda K, Ishikawa T, Iwashita K, Fujita N, Shimoi H. 2011. Whole-genome sequencing of sake yeast *Saccharomyces cerevisiae* Kyokai no. 7. DNA Res 18:423–434.
5. Watanabe D, Araki Y, Zhou Y, Maeya N, Akao T, Shimoi H. 2012. A loss-of-function mutation in the PAS kinase Rim15p is related to defective quiescence entry and high fermentation rates of *Saccharomyces cerevisiae* sake yeast strains. Appl Environ Microbiol 78:4008–4016.
6. Inai T, Watanabe D, Zhou Y, Fukada R, Akao T, Shima J, Takagi H, Shimoi H. 2013.

523 Rim15p-mediated regulation of sucrose utilization during molasses fermentation
524 using *Saccharomyces cerevisiae* strain PE-2. J Biosci Bioeng 116:591–594.
525 7. Watanabe D, Zhou Y, Hirata A, Sugimoto Y, Takagi K, Akao T, Ohya Y, Takagi H,
526 Shimoi H. 2016. Inhibitory role of Greatwall-like protein kinase Rim15p in alcoholic
527 fermentation via upregulating the UDP-glucose synthesis pathway in *Saccharomyces*
528 *cerevisiae*. Appl Environ Microbiol 82:340–351.
529 8. Oomuro M, Kato T, Zhou Y, Watanabe D, Motoyama Y, Yamagishi H, Akao T,
530 Aizawa M. 2016. Defective quiescence entry promotes the fermentation performance
531 of bottom-fermenting brewer's yeast. J Biosci Bioeng 122:577–582.
532 9. Watanabe D, Kaneko A, Sugimoto Y, Ohnuki S, Takagi H, Ohya Y. 2017. Promoter
533 engineering of the *Saccharomyces cerevisiae RIM15* gene for improvement of
534 alcoholic fermentation rates under stress conditions. J Biosci Bioeng 123:183–189.
535 10. Pedruzzi I, Dubouloz F, Cameroni E, Wanke V, Roosen J, Winderickx J, De Virgilio
536 C. 2003. TOR and PKA signaling pathways converge on the protein kinase Rim15 to
537 control entry into G_0. Mol Cell 12:1607–1613.
538 11. Wanke V, Pedruzzi I, Cameroni E, Dubouloz F, De Virgilio C. 2005. Regulation of
539 G_0 entry by the Pho80-Pho85 cyclin-CDK complex. EMBO J 24:4271–4278.
540 12. Panchaud N, Péli-Gulli MP, De Virgilio C. 2013. Amino acid deprivation inhibits
541 TORC1 through a GTPase-activating protein complex for the Rag family GTPase
542 Gtr1. Sci Signal 6:ra42.
543 13. Nicastro R, Sardu A, Panchaud N, De Virgilio C. 2017. The architecture of the Rag
544 GTPase signaling network. Biomolecules 7:48.
545 14. Tatebe H, Shiozaki K. 2017. Evolutionary conservation of the components in the

546 TOR signaling pathways. Biomolecules 7:77.

547 15. Urban J, Soulard A, Huber A, Lippman S, Mukhopadhyay D, Deloche O, Wanke V,
548 Anrather D, Ammerer G, Riezman H, Broach JR, De Virgilio C, Hall MN, Loewith R.
549 2007. Sch9 is a major target of TORC1 in *Saccharomyces cerevisiae*. Mol Cell
550 26:663–674.

551 16. Wanke V, Cameroni E, Uotila A, Piccolis M, Urban J, Loewith R, De Virgilio C.
552 2008. Caffeine extends yeast lifespan by targeting TORC1. Mol Microbiol 69:277–
553 285.

554 17. Chica N, Rozalén AE, Pérez-Hidalgo L, Rubio A, Novak B, Moreno S. 2016.
555 Nutritional control of cell size by the greatwall-endosulfine-PP2A·B55 pathway.
556 Curr Biol 26:319–330.

557 18. Düvel K, Yecies JL, Menon S, Raman P, Lipovsky AI, Souza AL, Triantafellow E,
558 Ma Q, Gorski R, Cleaver S, Vander Heiden MG, MacKeigan JP, Finan PM, Clish CB,
559 Murphy LO, Manning BD. 2010. Activation of a metabolic gene regulatory network
560 downstream of mTOR complex 1. Mol Cell 39:171–183.

561 19. Cameroni E, Hulo N, Roosen J, Winderickx J, De Virgilio C. 2004. The novel yeast
562 PAS kinase Rim15 orchestrates G_0-associated antioxidant defense mechanisms. Cell
563 Cycle 3:462–468.

564 20. Lee P, Kim MS, Paik SM, Choi SH, Cho BR, Hahn JS. 2013. Rim15-dependent
565 activation of Hsf1 and Msn2/4 transcription factors by direct phosphorylation in
566 *Saccharomyces cerevisiae*. FEBS Lett 587:3648–3655.

567 21. Yu J, Fleming SL, Williams B, Williams EV, Li Z, Somma P, Rieder CL, Goldberg
568 ML. 2004. Greatwall kinase: a nuclear protein required for proper chromosome

569 condensation and mitotic progression in *Drosophila*. J Cell Biol 164:487–492.

570 22. Mochida S, Maslen SL, Skehel M, Hunt T. 2010. Greatwall phosphorylates an
571 inhibitor of protein phosphatase 2A that is essential for mitosis. Science 330:1670–
572 1673.

573 23. Gharbi-Ayachi A, Labbé JC, Burgess A, Vigneron S, Strub JM, Brioudes E,
574 Van-Dorsselaer A, Castro A, Lorca T. 2010. The substrate of Greatwall kinase,
575 Arpp19, controls mitosis by inhibiting protein phosphatase 2A. Science 330:1673–
576 1677.

577 24. Bontron S, Jaquenoud M, Vaga S, Talarek N, Bodenmiller B, Aebersold R, De
578 Virgilio C. 2013. Yeast endosulfines control entry into quiescence and chronological
579 life span by inhibiting protein phosphatase 2A. Cell Rep 3:16–22.

580 25. Moreno-Torres M, Jaquenoud M, De Virgilio C. 2015. TORC1 controls G_1-S cell
581 cycle transition in yeast via Mpk1 and the greatwall kinase pathway. Nat Commun
582 6:8256.

583 26. Moreno-Torres M, Jaquenoud M, Péli-Gulli MP, Nicastro R, De Virgilio C. 2017.
584 TORC1 coordinates the conversion of Sic1 from a target to an inhibitor of
585 cyclin-CDK-Cks1. Cell Discov 3:17012.

586 27. Conrad M, Schothorst J, Kankipati HN, Van Zeebroeck G, Rubio-Texeira M,
587 Thevelein JM. 2014. Nutrient sensing and signaling in the yeast *Saccharomyces*
588 *cerevisiae*. FEMS Microbiol Rev. 38:254–299.

589 28. Takahara T, Maeda T. 2012. Transient sequestration of TORC1 into stress granules
590 during heat stress. Mol Cell 47:242–252.

591 29. Urano J, Sato T, Matsuo T, Otsubo Y, Yamamoto M, Tamanoi F. 2007. Point

592 mutations in TOR confer Rheb-independent growth in fission yeast and
593 nutrient-independent mammalian TOR signaling in mammalian cells. Proc Natl Acad
594 Sci U S A 104:3514–3519.
595 30. Ouchi K, Akiyama H, 1971. Non-foaming mutants of sake yeasts selection by cell
596 agglutination method and by froth flotation method. Agric Biol Chem 35:1024–1032.
597 31. Baro B, Játiva S, Calabria I, Vinaixa J, Bech-Serra JJ, de LaTorre C, Rodrigues J,
598 Hernáez ML, Gil C, Barceló-Batllori S, Larsen MR, Queralt E. 2018. SILAC-based
599 phosphoproteomics reveals new PP2A-Cdc55-regulated processes in budding yeast.
600 Gigascience 7:giy047.
601 32. Tripodi F, Nicastro R, Reghellin V, Coccetti P. 2015. Post-translational modifications
602 on yeast carbon metabolism: Regulatory mechanisms beyond transcriptional control.
603 Biochim Biophys Acta 1850:620–627.
604 33. Chen Y, Nielsen J. 2016. Flux control through protein phosphorylation in yeast.
605 FEMS Yeast Res 16:fow096.
606 34. Nakazawa N, Sato A, Hosaka M. 2016. TORC1 activity is partially reduced under
607 nitrogen starvation conditions in sake yeast Kyokai no. 7, *Saccharomyces cerevisiae*.
608 J Biosci Bioeng 121:247–252.
609 35. Oliveira AP, Ludwig C, Picotti P, Kogadeeva M, Aebersold R, Sauer U. 2012.
610 Regulation of yeast central metabolism by enzyme phosphorylation. Mol Syst Biol
611 8:623.
612 36. Goldstein AL, McCusker JH. 1999. Three new dominant drug resistance cassettes for
613 gene disruption in *Saccharomyces cerevisiae*. Yeast 15:1541–1553.
614 37. Janke C, Magiera MM, Rathfelder N, Taxis C, Reber S, Maekawa H,

615 Moreno-Borchart A, Doenges G, Schwob E, Schiebel E, Knop M. 2004. A versatile
616 toolbox for PCR-based tagging of yeast genes: new fluorescent proteins, more
617 markers and promoter substitution cassettes. Yeast 21:947–962.
618 38. Sato M, Dhut S, Toda T. 2005. New drug-resistant cassettes for gene disruption and
619 epitope tagging in *Schizosaccharomyces pombe*. Yeast 22:583–591.
620 39. Fujita M, Yamamoto M. 1998. *S. pombe sck2*$^{+}$, a second homologue of *S. cerevisiae*
621 *SCH9* in fission yeast, encodes a putative protein kinase closely related to PKA in
622 function. Curr Genet 33:248–254.
623 40. Kinoshita N, Ohkura H, Yanagida M. 1990. Distinct, essential roles of type 1 and 2A
624 protein phosphatases in the control of the fission yeast cell division cycle. Cell
625 63:405–415.
626 41. Kinoshita K, Nemoto T, Nabeshima K, Kondoh H, Niwa H, Yanagida M. 1996. The
627 regulatory subunits of fission yeast protein phosphatase 2A (PP2A) affect cell
628 morphogenesis, cell wall synthesis and cytokinesis. Genes Cells 1:29–45.
629 42. Watanabe D, Ota T, Nitta F, Akao T, Shimoi H. 2011. Automatic measurement of
630 sake fermentation kinetics using a multi-channel gas monitor system. J Biosci Bioeng
631 112:54–57.
632 43. Soga T, Heiger DN. 2000. Amino acid analysis by capillary electrophoresis
633 electrospray ionization mass spectrometry. Anal Chem 72:1236–1241.
634 44. Sugimoto M, Wong DT, Hirayama A, Soga T, Tomita M. 2000. Capillary
635 electrophoresis mass spectrometry-based saliva metabolomics identified oral, breast
636 and pancreatic cancer-specific profiles. Metabolomics 6:78–95.
637 45. Tanigawa M, Maeda T. 2017. An *in vitro* TORC1 kinase assay that recapitulates the

638 Gtr-independent glutamine-responsive TORC1 activation mechanism on yeast
639 vacuoles. Mol Cell Biol 37:e00075-17.
640 46. Kitamoto K, Oda K, Gomi K, Takahashi K. 1990. Construction of uracil and
641 tryptophan auxotrophic mutants from sake yeasts by disruption of *URA3* and *TRP1*
642 genes. Agric Bio Chem 54:2979–2987.
643 47. Nakazawa N, Abe K, Koshika Y, Iwano K. 2010. Cln3 blocks *IME1* transcription and
644 the Ime1-Ume6 interaction to cause the sporulation incompetence in a sake yeast,
645 Kyokai no. 7. J Biosci Bioeng 110:1–7.
646 48. Chia KH, Fukuda T, Sofyantoro F, Matsuda T, Amai T, Shiozaki K. 2017. Ragulator
647 and GATOR1 complexes promote fission yeast growth by attenuating TOR complex
648 1 through Rag GTPases. Elife 6:e30880.

FIGURE LEGENDS

FIG 1 Gene expression profiles downstream of TORC1: Comparison between a laboratory strain and a sake strain during sake fermentation. (A) Expression profiles of the ribosome-associated genes under the control of Sfp1p. (B) Expression profiles of genes belonging to the NCR and GAAC regulons. Expression levels in a laboratory strain (X2180) and a sake strain (K701) are derived from our previous DNA microarray data (3) and are indicated by red and blue, respectively. TORC1, target-of-rapamycin complex 1; NCR, nitrogen catabolite repression; GAAC, general amino acid control.

FIG 2 Effects of modification of the TORC1-Greatwall pathway on fermentation progression. Fermentation was monitored by measuring carbon dioxide emission. (A) Fermentation profiles of strain TM142 (wild type; gray) and its *rim15*Δ disruptant (red). (B) Fermentation profiles of strain TM142 in YPD20 medium in the absence (wild type, gray) or presence (red) of 1 nM rapamycin. (C to J) Fermentation profiles of strain TM142 (wild type; gray) and its *tor1*Δ (C), $TOR1^{L2134M}$ (D), $TOR2^{L2138M}$ (E), *gtr1*Δ (F), *gtr2*Δ (G), *npr2*Δ (H), *npr3*Δ (I), or *sch9*Δ (J) mutant (red). (K) Fermentation profiles of strain TM142 *rim15*Δ in YPD20 medium in the absence (*rim15*Δ; gray) or presence (red) of 1 nM rapamycin. (L) Fermentation profiles of strain TM142 *rim15*Δ (*rim15*Δ; gray) and its $TOR1^{L2134M}$ mutant (red). (M, N) Fermentation profiles of strain IB1401 (wild type; gray) and its *gtr1*Δ/*gtr1*Δ(M) or *sch9*Δ/*sch9*Δ (N) disruptant (blue). (O, P) Fermentation profiles of the wild-type *S. pombe* strain (wild type; gray) and its $tor2^{E2221K}$ (O) or *sck1/2*Δ (P) mutant (green). Fermentation tests were performed in YPD20 medium

672 (A to N) or in YPD10 medium (O, P) at 30°C for 5 d. Values represent the mean ± SD of
673 data from two or more independent experiments. *, significantly different from the value
674 for the control experiment (*t* test, $P < 0.05$). Note that the experiments using laboratory,
675 sake, and fission yeast strains are indicated in red, blue, and green, respectively. WT, wild
676 type; Rap, rapamycin.
677
678 **FIG 3** Effects of modification of the Greatwall-PP2A$^{B55\delta}$ pathway on fermentation
679 progression. Fermentation was monitored by measuring carbon dioxide emission. (A, B)
680 Fermentation profiles of strain BY4741 (wild type; gray) and its *rim15*Δ (A) or *igo1/2*Δ
681 (B) disruptant (red). (C, D) Fermentation profiles of the wild-type *S. pombe* strain (wild
682 type; gray) and its *cek1*Δ*/ppk18*Δ (C) or *igo1*Δ (D) disruptant (green). (E to I)
683 Fermentation profiles of strain BY4741 (wild type; gray) and its *pph21*Δ (E), *pph22*Δ (F),
684 *tpd3*Δ (G), *cdc55*Δ (H), or *rts1*Δ (I) disruptant (red). (J to L) Fermentation profiles of the
685 wild-type *S. pombe* strain (wild type; gray) and its *ppa1*Δ (J), *ppa2*Δ (K) or *pab1*Δ (L)
686 disruptant (green). (M, N) Fermentation profiles of strain BY4741 *cdc55*Δ (*cdc55*Δ; gray)
687 and its *rim15*Δ (M) or *igo1/2*Δ (N) disruptant (red). (O) Fermentation profiles of the *S.*
688 *pombe pab1*Δ strain (*pab1*Δ; gray) and its *igo1*Δ disruptant (green). (P) Fermentation
689 profiles of strain K701 UT-1T with an empty vector (wild type; gray) and with a
690 functional *RIM15*-expressing plasmid (blue). (Q, R) Fermentation profiles of strain K701
691 (wild type; gray) and its *CDC55*^{WT}*/cdc55*^{MT}Δ (Q) or *cdc55*^{WT}Δ*/cdc55*^{MT} (N) disruptant
692 (blue). Fermentation tests were performed in YPD20 medium (A, B, E to I, M, N, P to R)
693 or in YPD10 medium (C, D, J to L, O) at 30°C for 5 d. Values represent the mean ± SD of
694 data from two or more independent experiments. *, significantly different from the value

695 for the control experiment (*t* test, $P < 0.05$). Note that the experiments using laboratory,
696 sake, and fission yeast strains are indicated by red, blue, and green, respectively. WT,
697 wild type.
698
699 **FIG 4** Heterozygous nonsense or frameshift mutations found in the *CDC55* genes of
700 K7-related sake strains. (A) The $cdc55^{1092delA}$ (a.k.a. $cdc55^{MT}$) mutation unique to K701.
701 In this loss-of-function allele of K701, deletion of a single adenine nucleotide at ORF
702 nucleotide 1092 causes a premature stop codon. (B) Mutation sites of the *CDC55* gene of
703 K7-related sake strains. Nonsense and frameshift mutation sites are indicated by pink and
704 orange dots, respectively. fs, frameshift.
705
706 **FIG 5** Effects of Cdc55p on glycolytic intermediate levels in the early stage of alcoholic
707 fermentation. (A to C) Intracellular metabolite levels of laboratory strain BY4741 *cdc55*Δ
708 at 6 h (A), 1 d (B), and 2 d (C) from the onset of alcoholic fermentation; values are
709 normalized to those of the BY4741 wild type at the respective time point. (D)
710 Intracellular metabolite levels of sake strain K701 $cdc55^{WT}\Delta/cdc55^{MT}$ at 1 d from the
711 onset of alcoholic fermentation; values are normalized to those of K701
712 $CDC55^{WT}/cdc55^{MT}\Delta$. Red and blue arrows indicate notable differences between adjacent
713 metabolites. Data provided are from a single experiment representative of results from
714 multiple independent fermentation tests. G6P, glucose 6-phosphate; F6P, fructose
715 6-phosphate; F1,6BP, fructose 1,6-bisphosphate; DHAP, dihydroxyacetone phosphate;
716 G3P, glyceraldehyde 3-phosphate; 3PG, 3-phosphoglyceric acid; 2PG, 2-phosphoglyceric
717 acid; PEP, phosphoenolpyruvic acid; Pyr, pyruvic acid; n.d., not determined. Note that

718 G3P was not detected in K701 *cdc55*^{WT}Δ/*cdc55*^{MT}, and that 1,3-bisphosphoglyceric acid
719 (1,3BPG) was not detected in any of the samples.
720
721 **FIG 6** A hypothetical model of the regulation of fermentation control by the
722 TORC1-Greatwall-PP2A$^{B55\delta}$ pathway. Orange and green colors indicate higher and lower
723 activities, respectively, than those of *S. cerevisiae* wild-type laboratory strains. (A) In *S.*
724 *cerevisiae* laboratory strains and *S. pombe*, changes in the activity of TORC1, Greatwall,
725 or PP2A$^{B55\delta}$ may lead to altered alcoholic fermentation performance. (B) In *S. cerevisiae*
726 sake strains, both the high TORC1 activity and the loss of Rim15p may contribute to the
727 constitutively high PP2A$^{B55\delta}$ activity. Thus, PP2A$^{B55\delta}$ must be disrupted to impair the
728 fermentation performance in these strains.

Fig. 1 (Watanabe *et al.*)

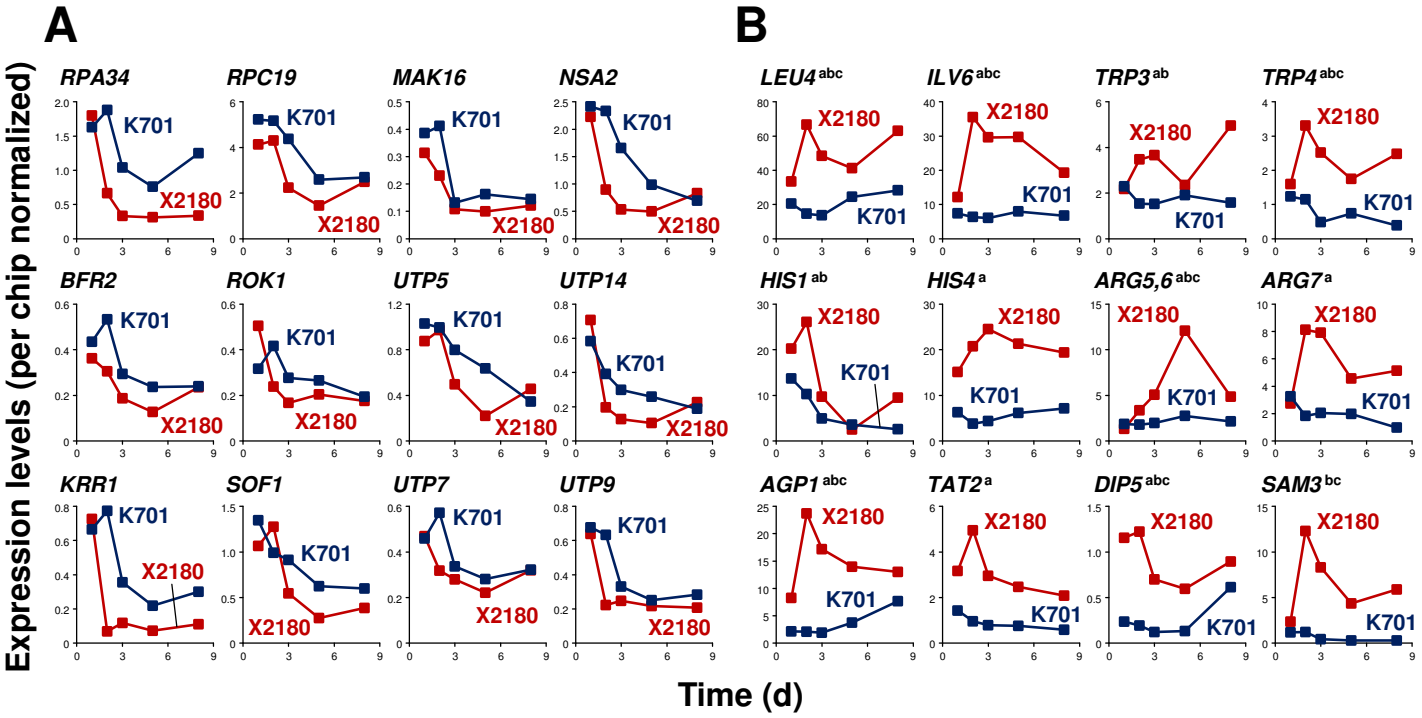

FIG 1 Gene expression profiles downstream of TORC1: Comparison between a laboratory strain and a sake strain during sake fermentation. (A) Expression profiles of the ribosome-associated genes under the control of Sfp1p. (B) Expression profiles of genes belonging to the NCR and GAAC regulons. Expression levels in a laboratory strain (X2180) and a sake strain (K701) are derived from our previous DNA microarray data (3) and are indicated by red and blue, respectively. TORC1, target-of-rapamycin complex 1; NCR, nitrogen catabolite repression; GAAC, general amino acid control.

Fig. 2 (Watanabe *et al.*)

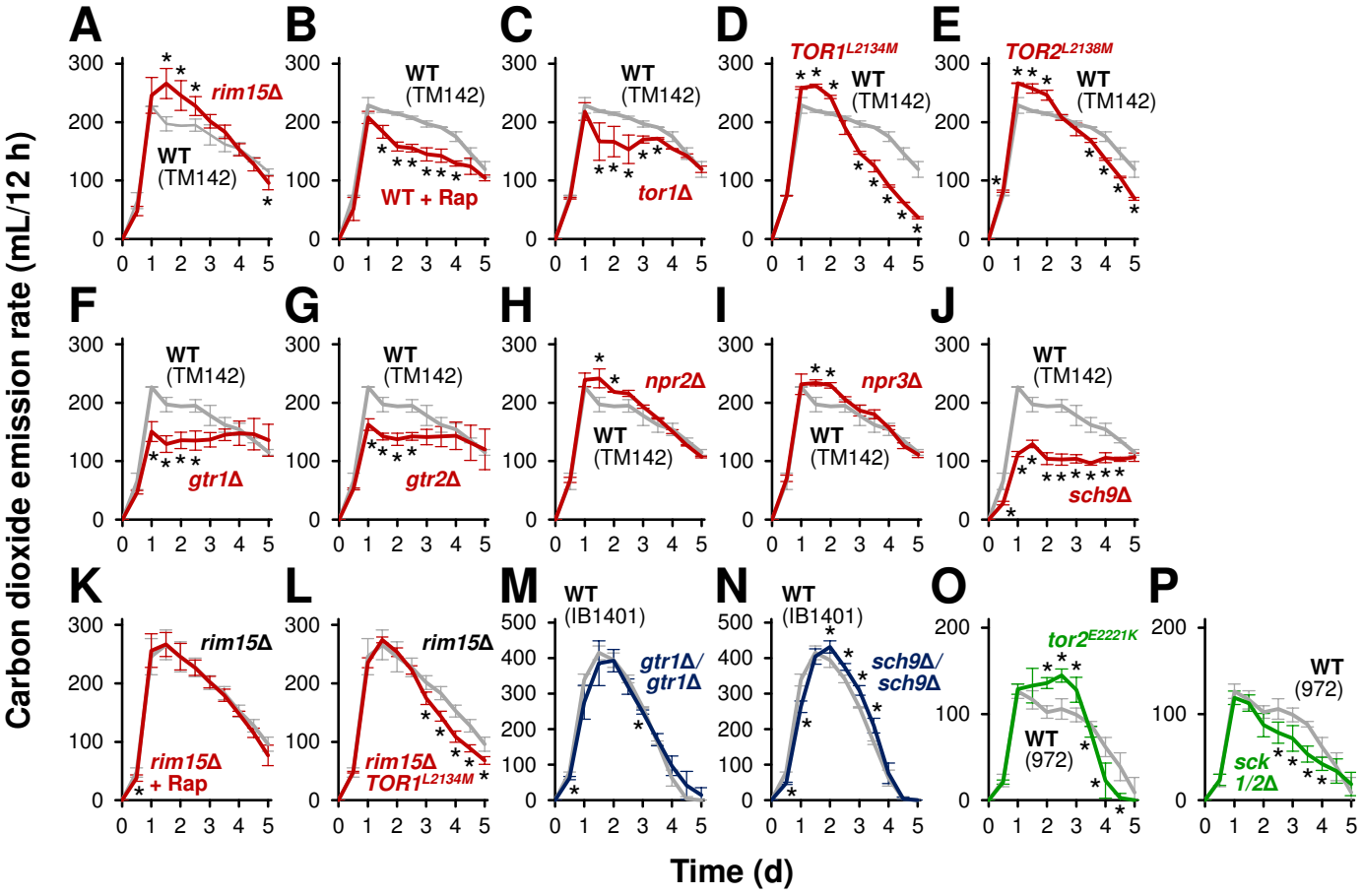

FIG 2 Effects of modification of the TORC1-Greatwall pathway on fermentation progression. Fermentation was monitored by measuring carbon dioxide emission. (A) Fermentation profiles of strain TM142 (wild type; gray) and its *rim15*Δ disruptant (red). (B) Fermentation profiles of strain TM142 in YPD20 medium in the absence (wild type, gray) or presence (red) of 1 nM rapamycin. (C to J) Fermentation profiles of strain TM142 (wild type; gray) and its *tor1*Δ (C), *TOR1*^{L2134M} (D), *TOR2*^{L2138M} (E), *gtr1*Δ (F), *gtr2*Δ (G), *npr2*Δ (H), *npr3*Δ (I), or *sch9*Δ (J) mutant (red). (K) Fermentation profiles of strain TM142 *rim15*Δ in YPD20 medium in the absence (*rim15*Δ; gray) or presence (red) of 1 nM rapamycin. (L) Fermentation profiles of strain TM142 *rim15*Δ (*rim15*Δ; gray) and its *TOR1*^{L2134M} mutant (red). (M, N) Fermentation profiles of strain IB1401 (wild type; gray) and its *gtr1*Δ/*gtr1*Δ(M) or *sch9*Δ/*sch9*Δ (N) disruptant (blue). (O, P) Fermentation profiles of the wild-type *S. pombe* strain (wild type; gray) and its *tor2*^{E2221K} (O) or *sck1/2*Δ (P) mutant (green). Fermentation tests were performed in YPD20 medium (A to N) or in YPD10 medium (O, P) at 30° C for 5 d. Values represent the mean ± SD of data from two or more independent experiments. *, significantly different from the value for the control experiment (*t* test, $P < 0.05$). Note that the experiments using laboratory, sake, and fission yeast strains are indicated in red, blue, and green, respectively. WT, wild type; Rap, rapamycin.

Fig. 3 (Watanabe *et al.*)

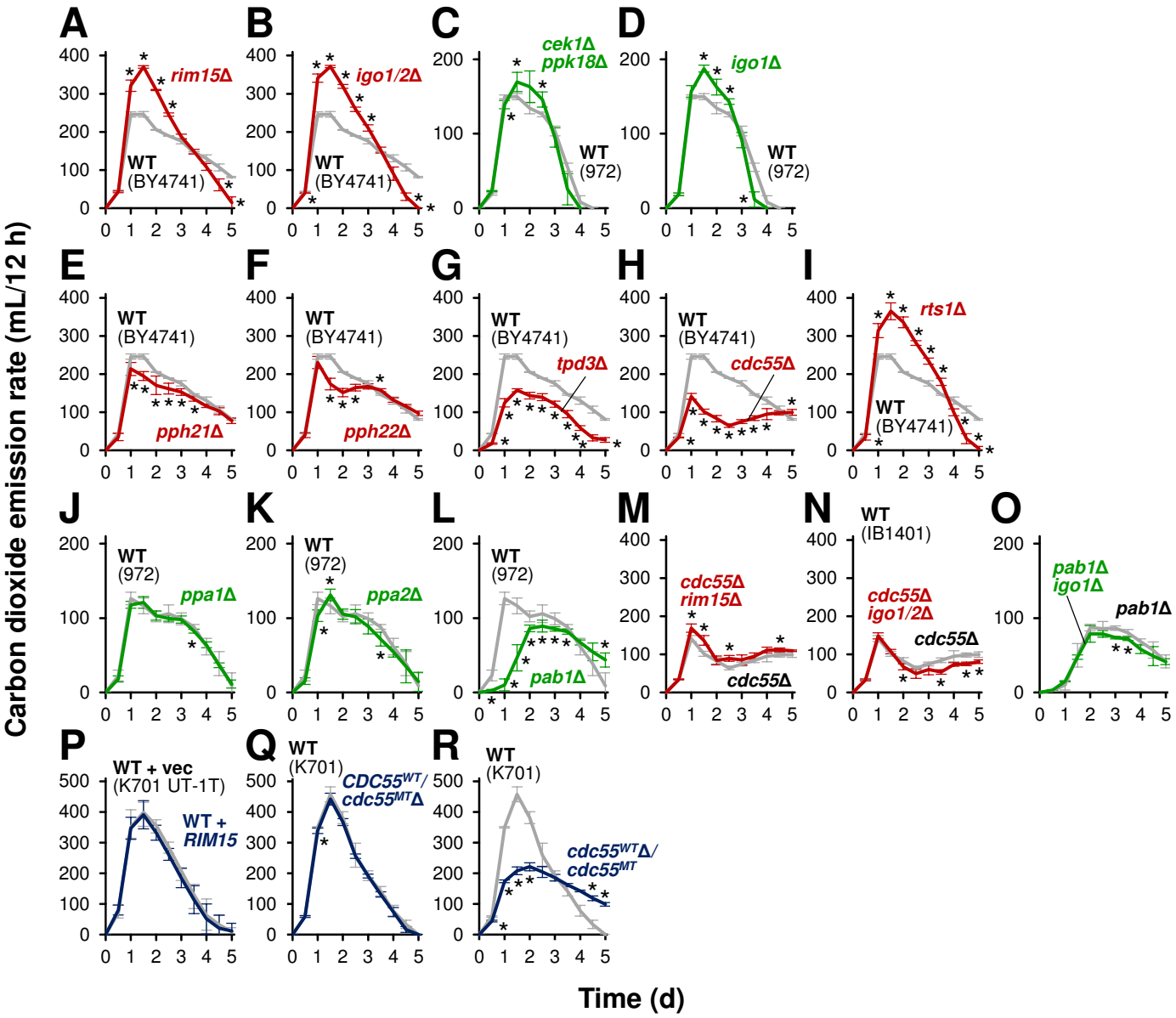

FIG 3 Effects of modification of the Greatwall-PP2A$^{B55\delta}$ pathway on fermentation progression. Fermentation was monitored by measuring carbon dioxide emission. (A, B) Fermentation profiles of strain BY4741 (wild type; gray) and its *rim15*Δ (A) or *igo1/2*Δ (B) disruptant (red). (C, D) Fermentation profiles of the wild-type *S. pombe* strain (wild type; gray) and its *cek1*Δ*/ppk18*Δ (C) or *igo1*Δ (D) disruptant (green). (E to I) Fermentation profiles of strain BY4741 (wild type; gray) and its *pph21*Δ (E), *pph22*Δ (F), *tpd3*Δ (G), *cdc55*Δ (H), or *rts1*Δ (I) disruptant (red). (J to L) Fermentation profiles of the wild-type *S. pombe* strain (wild type; gray) and its *ppa1*Δ (J), *ppa2*Δ (K) or *pab1*Δ (L) disruptant (green). (M, N) Fermentation profiles of strain BY4741 *cdc55*Δ (*cdc55*Δ; gray) and its *rim15*Δ (M) or *igo1/2*Δ (N) disruptant (red). (O) Fermentation profiles of the *S. pombe pab1*Δ strain (*pab1*Δ; gray) and its *igo1*Δ disruptant (green). (P) Fermentation profiles of strain K701 UT-1T with an empty vector (wild type; gray) and with a functional *RIM15*-expressing plasmid (blue). (Q, R) Fermentation profiles of strain K701 (wild type; gray) and its *CDC55*^{WT}*/cdc55*^{MT}Δ (Q) or *cdc55*^{WT}Δ*/cdc55*^{MT} (N) disruptant (blue). Fermentation tests were performed in YPD20 medium (A, B, E to I, M, N, P to R) or in YPD10 medium (C, D, J to L, O) at 30° C for 5 d. Values represent the mean ± SD of data from two or more independent experiments. *, significantly different from the value for the control experiment (*t* test, $P < 0.05$). Note that the experiments using laboratory, sake, and fission yeast strains are indicated by red, blue, and green, respectively. WT, wild type.

Fig. 4 (Watanabe *et al.*)

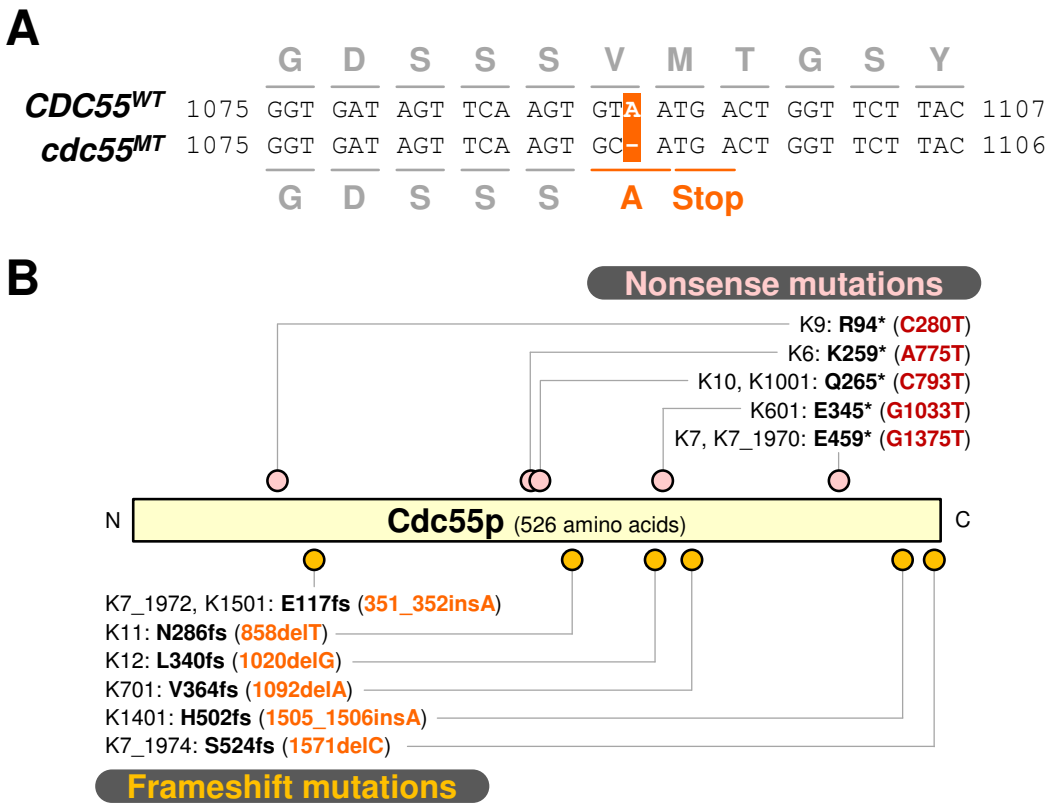

FIG 4 Heterozygous nonsense or frameshift mutations found in the *CDC55* genes of K7-related sake strains. (A) The *cdc55*^{1092delA} (a.k.a. *cdc55*^{MT}) mutation unique to K701. In this loss-of-function allele of K701, deletion of a single adenine nucleotide at ORF nucleotide 1092 causes a premature stop codon. (B) Mutation sites of the *CDC55* gene of K7-related sake strains. Nonsense and frameshift mutation sites are indicated by pink and orange dots, respectively. fs, frameshift.

Fig. 5 (Watanabe *et al.*)

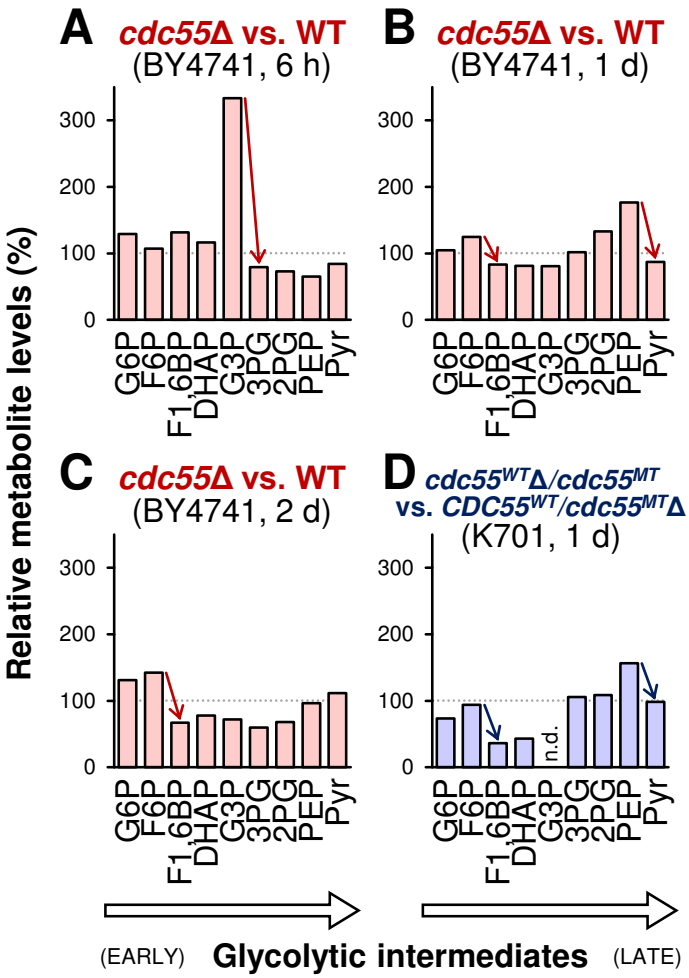

FIG 5 Effects of Cdc55p on glycolytic intermediate levels in the early stage of alcoholic fermentation. (A to C) Intracellular metabolite levels of laboratory strain BY4741 *cdc55*Δ at 6 h (A), 1 d (B), and 2 d (C) from the onset of alcoholic fermentation; values are normalized to those of the BY4741 wild type at the respective time point. (D) Intracellular metabolite levels of sake strain K701 $cdc55^{WT}\Delta/cdc55^{MT}$ at 1 d from the onset of alcoholic fermentation; values are normalized to those of K701 $CDC55^{WT}/cdc55^{MT}\Delta$. Red and blue arrows indicate notable differences between adjacent metabolites. Data provided are from a single experiment representative of results from multiple independent fermentation tests. G6P, glucose 6-phosphate; F6P, fructose 6-phosphate; F1,6BP, fructose 1,6-bisphosphate; DHAP, dihydroxyacetone phosphate; G3P, glyceraldehyde 3-phosphate; 3PG, 3-phosphoglyceric acid; 2PG, 2-phosphoglyceric acid; PEP, phosphoenolpyruvic acid; Pyr, pyruvic acid; n.d., not determined. Note that G3P was not detected in K701 $cdc55^{WT}\Delta/cdc55^{MT}$, and that 1,3-bisphosphoglyceric acid (1,3BPG) was not detected in any of the samples.

Fig. 6 (Watanabe *et al.*)

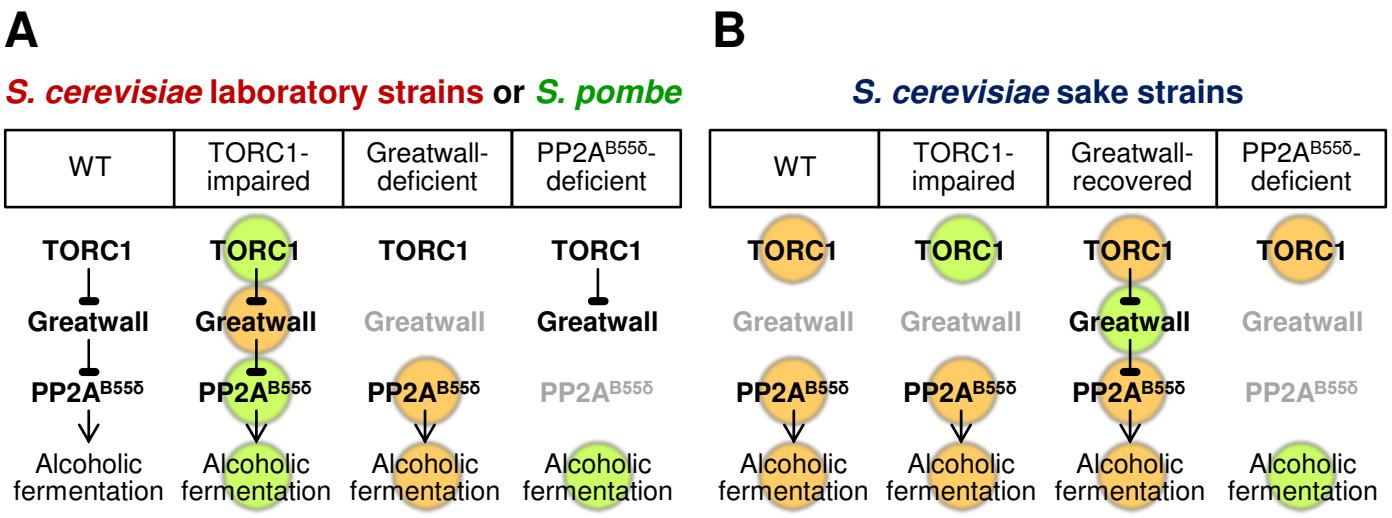

FIG 6 A hypothetical model of the regulation of fermentation control by the TORC1-Greatwall-PP2A$^{B55\delta}$ pathway. Orange and green colors indicate higher and lower activities, respectively, than those of *S. cerevisiae* wild-type laboratory strains. (A) In *S. cerevisiae* laboratory strains and *S. pombe*, changes in the activity of TORC1, Greatwall, or PP2A$^{B55\delta}$ may lead to altered alcoholic fermentation performance. (B) In *S. cerevisiae* sake strains, both the high TORC1 activity and the loss of Rim15p may contribute to the constitutively high PP2A$^{B55\delta}$ activity. Thus, PP2A$^{B55\delta}$ must be disrupted to impair the fermentation performance in these strains.